ELSEVIER

Contents lists available at ScienceDirect

Physics of the Earth and Planetary Interiors

journal homepage: www.elsevier.com/locate/pepi



Compressibility of the 23 Å phase under high pressure and high temperature

Check for updates

Nao Cai^{a,*}, Takumi Kikegawa^b, Toru Inoue^{a,c,d}

- ^a Geodynamics Research Center, Ehime University, Matsuyama, Ehime 790-8577, Japan
- ^b Photon Factory, High Energy Accelerator Research Organization, Tsukuba, Ibaraki 305-0801, Japan
- ^c Department of Earth and Planetary Systems Science, Graduate School of Science, Hiroshima University, Higashi-Hiroshima, Hiroshima 739-8526, Japan
- d Hiroshima Institute of Plate Convergence Region Research (HiPeR), Hiroshima University, Higashi-Hiroshima, Hiroshima 739-8526, Japan

ARTICLE INFO

Keywords: 23 Å phase Equation of state Hydrous phases Upper mantle

ABSTRACT

A new Al-bearing high-pressure hydrous Mg-silicate named 23 Å phase with a hexagonal structure, which is stable in chlorite composition and could be an important water carrier in the subducting slab, was reported by Cai et al. (2015a). Here, for the first time, we determined the equation of state of the 23 Å phase up to 10 GPa and 1073 K by energy-dispersive *in situ* X-ray diffraction. Fitting the *P-V* data to the room temperature Birch-Murnaghan equation of state yielded $V_0 = 538.0(3)$ Å and $K_0 = 111(1)$ GPa by fixing K' at 4. The high temperature 3rd order Birch-Murnaghan equation of state was used to fit the *P-V-T* data, yielding $V_0 = 538.0(3)$ Å 3 , $K_0 = 109(1)$ GPa, $\partial K/\partial T = -0.012(5)$ GPa/K, and $a_0 = 3.0(4) \times 10^{-5}$ /K by fixing K' at 4. Very little anisotropy was observed, and the axial compressibilities were 2.54(2) 10^{-3} /GPa for the a axis and $a_0 = 3.0(4) \times 10^{-5}$ /K by fixing $a_0 = 3.0(4) \times 10^{-3}$ /GPa for the $a_$

1. Introduction

Dense hydrous phases are believed to transport water into deep Earth through subduction processes (Ohtani et al., 2004; Ono, 1998; Schmidt and Poli, 1998). Previous results have shown that serpentine is the dominant hydrous phase in the upper part of the subducting slabs (e.g., Cannat et al., 1995; Komabayashi et al., 2005). Irifune et al. (1998) and Inoue et al. (2009) have reported that at high pressure (> 5 GPa) and relatively low temperature (below 600–800 °C), serpentine will decompose into phase A and the 10 Å phase (or talc), and phase A was believed to be the major hydrous phase in the deeper part of the subducting slabs. On the other hand, in the Al-bearing subduction zones, chlorite is another predominant hydrous phase (e.g. Bebout, 2007; Spandler et al., 2008) at shallow depths.

Recently, we reported a new Al-bearing hydrous phase named the $23\,\text{Å}$ phase $(\text{Mg}_{11}\text{Al}_2\text{Si}_4\text{O}_{16}(\text{OH})_{12})$ (Cai et al., 2015a), which forms after the breakdown of a natural chlorite sample. In addition, the chemical composition and stability region of the $23\,\text{Å}$ phase suggest that it should replace phase A to be the dominant hydrous phase in an Al-bearing subducting slab, as phase A can only contain less than 0.5 wt % Al. Despite the lack of crystal structure data for this $23\,\text{Å}$ phase, the

symmetry information obtained in the present study allowed us to establish its equation of state by assuming a simplified hexagonal structure, as all of the peaks (except those that can be identified as pyrope, MgO and hBN) can be indexed using such symmetry. Thus, in this study, for the first time, we establish the high-pressure and high-temperature equation of state of this 23 Å phase up to 10 GPa and 1073 K in order to further improve the mineralogical models of the hydrous subducted slab.

2. Experimental methods

The powder sample was synthesized using a Kawai type multi-anvil apparatus driven by a 3000-ton uniaxial press. The starting material was the stoichiometric mixture of reagent grade MgO, Al_2O_3 , SiO_2 and Mg(OH)₂. The mixture was loaded into a Pt capsule and then heated to $1000\,^{\circ}\text{C}$ at $10\,\text{GPa}$ for $10\,\text{h}$. The run product was then crushed into fine powder and identified by X-ray diffraction (XRD) as almost pure $23\,\text{Å}$ phase with a small amount of pyrope. Fitting the powder diffraction pattern of the $23\,\text{Å}$ phase yielded $a_0 = 5.199(1)\,\text{Å}$, $c_0 = 22.974(4)\,\text{Å}$ and $V_0 = 537.9(3)\,\text{Å}^3$ at ambient conditions, which are consistent with the parameters reported by Cai et al. (2015a).

^{*} Corresponding author at: Stony Brook University, 130 Earth and Space Sciences Building, Stony Brook, NY 11794-2100, USA. *E-mail address*: nao.cai@stonybrook.edu (N. Cai).

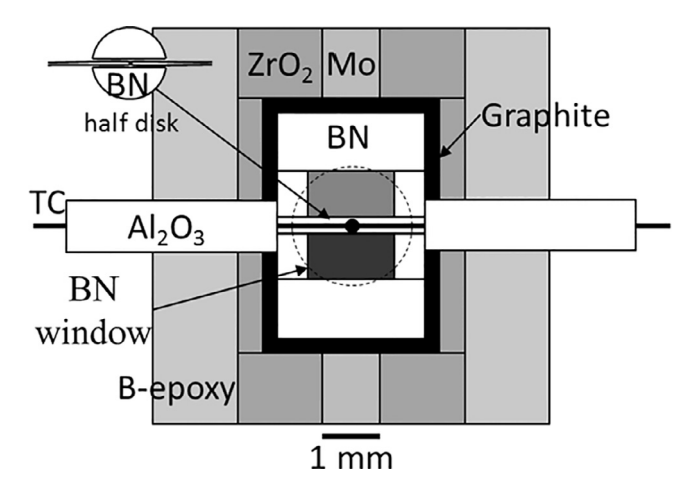


Fig. 1. 7/4 cell assembly used in our in situ X-ray experiments.

High pressure and high temperature *in situ* synchrotron X-ray experiments were conducted using a cubic type multi-anvil apparatus (MAX80) installed at the NE5C beamline in PF-AR of KEK, Tsukuba, Japan, which adopts the 6-6 type compression system. The technical details of the 6-6 type MA and X-ray optical system of the beamline were described by Nishiyama et al. (2008) and Yang et al. (2014), respectively.

In the *in situ* experiments, 7/4 and 9/6 cells (pressure medium size/truncation edge length in mm) were used. A typical 7/4 cell assembly is shown in Fig. 1. We used boron epoxy as the pressure medium and graphite as the heater. The temperature was measured using a $W_{97\%}Re_{3\%}$ - $W_{75\%}Re_{25\%}$ thermocouple (0.1 mm diameter), which was placed between 0.3 mm thick BN spacers to avoid reaction between the sample and the pressure marker. A mixture of NaCl and Au at the weight ratio of 10:1 was used as the pressure marker, with which the pressures were calculated using the equation of state (EoS) of NaCl (Decker, 1971).

The pressure and temperature paths for data collection are shown in Fig. 2. The cell was compressed to the target pressure and then heated to the target temperature (873, 973 or 1073 K, depending on the pressure) within the stability region to release the deviatoric stress. The diffraction patterns were obtained at every 100 K in the cooling process until room temperature. The lattice parameters of the pressure marker were derived using the XrayAnalysis software provided by PF-KEK for the NE5C beamline, and the lattice parameters of the sample were

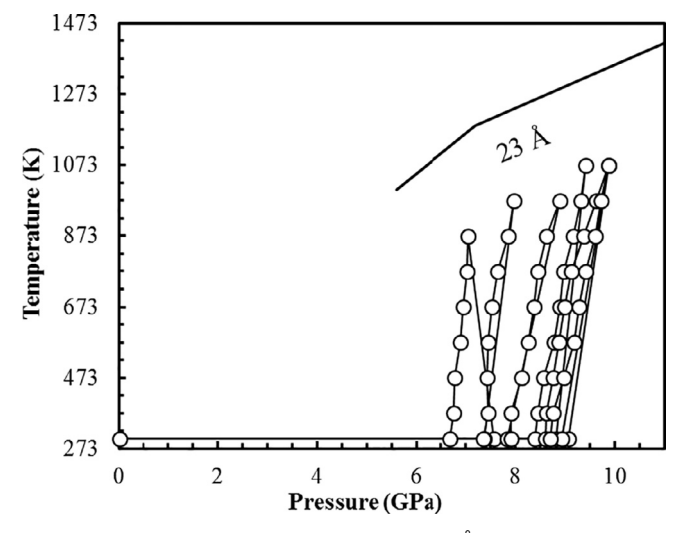


Fig. 2. P-T paths in the *in situ* experiments of the 23 Å phase. Solid line shows the high temperature stability limit of the 23 Å phase (Cai et al., 2015a).

derived by PDIndexer software, which is the powder diffraction fitting program developed by Y. Seto (see http://pmsl.planet.sci.kobe-u.ac.jp/~seto/?page_id=20&lang=en). The lattice parameters of the sample were carefully determined by measuring the positions of at least 13 strong and isolated peaks in the diffraction patterns.

3. Results and discussions

Based on our newly obtained results, the ideal formula of the 23 Å phase must be modified for the following reasons: 1) preliminary single crystal results suggest that the number of oxygen atoms in this unit cell should be 30 instead of the 28 suggested in Cai et al. (2015a); 2) density measurement of a bulk sample synthesized at 10 GPa and 1273 K, mostly containing the 23 Å phase with approximately 5 vol% of pyrope, suggests a density of 2.930 g/cm³ for the 23 Å phase, which is larger than that previously proposed by us (Cai et al., 2015a). Thus, by revaluating the measured chemical compositions, the ideal formula of the 23 Å phase is obtained as $Mg_{12}Al_2Si_4O_{16}(OH)_{14}$, with the calculated density of 2.941 g/cm³ and water content of 13.2 wt%, assuming the same cell volume as that in Cai et al. (2015a). This corrected density is similar to that of the 11.5 Å phase reported by Gemmi et al. (2016) recently, which was discovered at 6.5 GPa and 973 K. The single crystal results will be discussed in greater detail in a separate paper.

No phase transformation or decomposition of the 23 Å phase was observed throughout the experiments. The unit-cell volume of the 23 Å phase shows a continuous decrease with increasing pressure in the pressure range of 6–9 GPa (Fig. 3) at room temperature and is 537.5(3) Å at ambient conditions after releasing the pressure. The room temperature P-V data (see Table 1) were fitted by a third order Birch-Murnaghan equation of state (BM EoS):

$$P = \frac{3}{2}K_0 \left[\left(\frac{V_0}{V} \right)^{\frac{7}{3}} - \left(\frac{V_0}{V} \right)^{\frac{5}{3}} \right] \left\{ 1 + \frac{3}{4} (K_0' - 4) \left[\left(\frac{V_0}{V} \right)^{\frac{2}{3}} - 1 \right] \right\}$$
 (1)

where V_0 , K_0 and K'_0 are the unit cell volume, isothermal bulk modulus, and its pressure derivative at ambient conditions, respectively. K'_0 was fixed at 4 due to the few data points used for the fit. The unit cell volume and the bulk modulus of the 23 Å phase at ambient conditions were determined to be $V_0 = 538.0(3)$ Å³ and $K_0 = 111(1)$ GPa, respectively.

Fig. 3 shows the compressibility of the 23 Å phase at room temperature compared to those of phase A (Kuribayashi et al., 2003), the

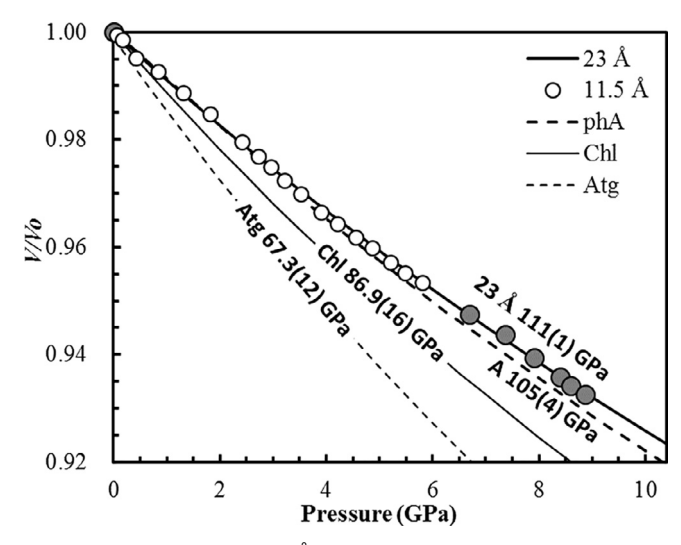


Fig. 3. Compressibility of the 23 Å phase (solid circles) at room temperature, compared to those of the 11.5 Å phase (open circles; Gemmi et al., 2016), phase A (phA, thick dashed line; Kuribayashi et al., 2003), chlorite (Chl, thin solid line; Pawley et al., 2002) and antigorite (Atg, thin dashed line; Hilairet et al., 2006).

Download English Version:

https://daneshyari.com/en/article/8915648

Download Persian Version:

https://daneshyari.com/article/8915648

<u>Daneshyari.com</u>